Optical Properties of Gold and α-Phase Gold-Aluminum Alloys*

G. B. Irani,† T. Huen, and F. Wooten
Department of Applied Science and Lawrence Livermore Laboratory, University of California, Livermore, California 94550
(Received 3 April 1972)

Reflectance measurements at nearly normal incidence were used to investigate the optical properties and electronic band structure of gold and dilute alloys of aluminum in gold. Sample films were prepared, maintained, and measured in ultrahigh vacuum with base pressures less than 10^{-9} Torr. Measurements were made in the spectral range 1.1 – 11.5 eV. Shifts in the ϵ_2 peak at 3.09 eV ($L_3 \rightarrow L_{2'}$) are at one-half the rate expected for the rigid-band model. The change in most transitions upon alloying is consistent with previous assignments. There appears to be a downward shift of $X_{4'}$ with respect to the d bands.

I. INTRODUCTION

The optical studies reported here are an extension of earlier studies on pure silver and α-phase Ag-Al alloys.[1] The extension is a natural one. Aluminum has the same crystal structure (fcc) and nearly the same lattice spacing (4.05 Å) as both silver (4.09 Å) and gold (4.08 Å). Thus when silver or gold atoms are replaced by aluminum atoms, little distortion of the lattice occurs, and change in the free energy of the alloy depends largely on electronic levels. Aluminum has no d states of its own to contribute to the valence band of the alloy. It acts to shift and broaden structure related to the gold or silver matrix. It is the direction of shift in optical structure that aids in correlating optical transitions with electronic-band-structure calculations. The magnitude of shifts in transitions to or from the Fermi surface serves as a check on the validity of the rigid-band model of Mott and Jones,[2] Friedel's model[3] of dilute alloys, or the recent theory of Stern.[4,5] The experiments on Ag-Al alloys suggested that the true description for Ag-Al alloys lies somewhere between the theories of Friedel and Stern. The present experiments on Au-Al alloys were aimed at seeing if this picture is more generally valid.

II. EXPERIMENTAL

Alloys of Au-Al were prepared from high-purity constituents (99.999%) in a demountable vacuum system with a base pressure less than 10^{-6} Torr. Slugs of these alloys, along with slugs of pure gold, were then evaporated in an ultrahigh-vacuum chamber (base pressure $< 10^{-9}$ Torr) to form films of highly specular and uniform reflectance. The evaporated films (5000-Å average thickness) were annealed for 10–14 h at temperatures near 320 °C. Annealing is important. For example, the structure in the reflectance of gold between 8 and 10 eV, as shown in Fig. 1, is difficult to discern prior to annealing. The corresponding structure for the alloys could be lost entirely.

Further details of sample preparation are given in the earlier paper on Ag-Al alloys.[1] The same procedures were used for the Au-Al alloys discussed here.

The ultrahigh vacuum chamber used for film evaporation also served as the reflectometer chamber. Thus, the samples were prepared and maintained, and reflectances measured, under ultrahigh vacuum conditions. The reflectometer system permits continuous measurement and recording of the reflectance as the wavelength is slowly but automatically scanned.[1,6] The monochromator and light sources were the same as those used previously for studies of Ag-Al alloys.[1]

Reflectance measurements were made at both 300 and 100 °K. Figures 1 and 2 show the mea-

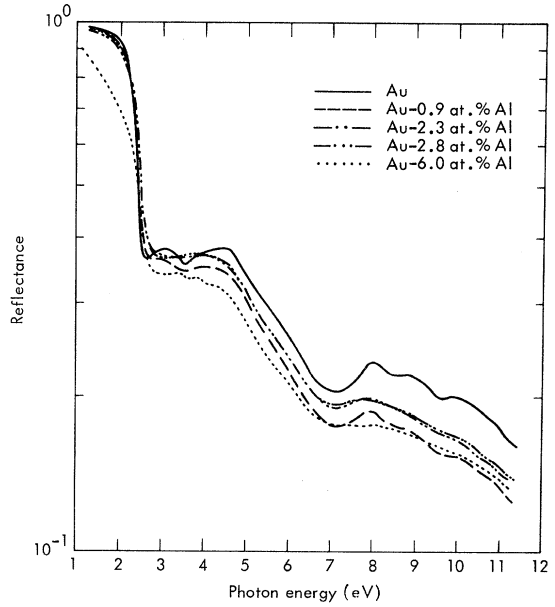

FIG. 1. Comparison of gold and gold-aluminum reflectances at 300 °K.

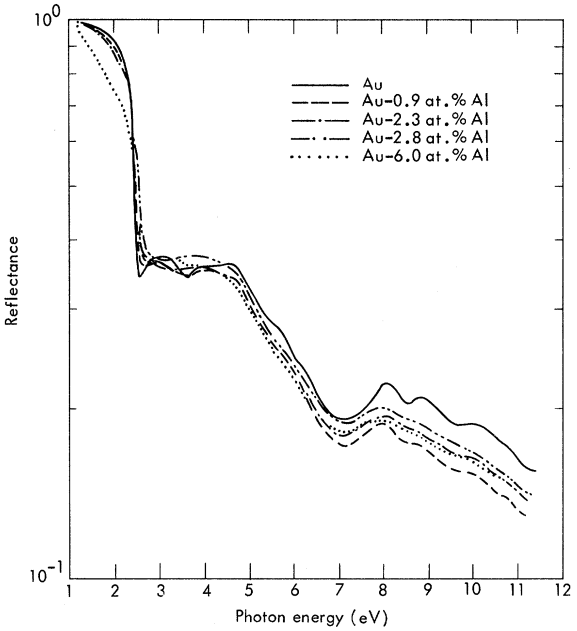

FIG. 2. Comparison of gold and gold-aluminum reflectances at 100 °K.

sured reflectance curves for gold and a series of Au-Al alloys at these temperatures. Note that the major effect of cooling is simply to sharpen structure, not to shift it. However, there are shifts in structure upon alloying. These shifts are most clearly seen in plots of $\epsilon_2(\omega)$ and are discussed later.

III. DATA ANALYSIS

The optical constants ϵ_1 and ϵ_2 were determined from a Kramers–Kronig analysis of reflectance data. The method requires an integration over the entire spectrum to determine the phase change on reflectance. Thus, extrapolations are required for spectral regions outside the range of experimental data. For gold and Au-Al alloys, the reflectance approaches 1.0 as $\hbar\omega \to 0$, and a linear extrapolation between the measured reflectance at $\hbar\omega = 1.1$ eV and the theoretical reflectance of unity at $\hbar\omega = 0$ is quite satisfactory. Our own data were used in the range $1.1 \leq \hbar\omega \leq 11$ eV. The data of other workers (as compiled by Cooper *et al.*[7]) were used for gold in the range $11 \leq \hbar\omega \leq 45$ eV. The Au-Al alloys were assumed to have the same form of spectral reflectance as pure gold in the range $11 \leq \hbar\omega \leq 45$ eV. In the range $45 \leq \hbar\omega \leq 100$ eV, the empirical power law

$$R(\omega) = R_{45}\,(\omega/\omega_{45})^{-8.07} \qquad (1)$$

was used. The reflectance at $\hbar\omega = 45$ eV is R_{45} and the corresponding angular frequency is ω_{45}. Above 100 eV, the reflectance was taken to follow the asymptotic free-electron behavior

$$R(\omega) = R_{100}\,(\omega/\omega_{100})^{-4} \quad , \qquad (2)$$

where R_{100} is the reflectance at $\hbar\omega = 100$ eV as determined from Eq. (1) and ω_{100} is the corresponding angular frequency.

Although an empirically fit power-law extrapolation fails to allow for nonmonotonic behavior in the reflectance, it has been applied with reasonable success to the noble metals.[7,8] The exponents in Eqs. (1) and (2) were chosen in a manner suggested by Cooper *et al.*[7] that gives best agreement with the reflectance data of other workers at high energy and with the absorption measurements of Haensel *et al.*[9] The present analysis differs from the previous analysis for silver and Ag-Al alloys in that two parameters are used here to give a best fit for gold and Au-Al alloys. It was impossible to improve the analysis of silver and Ag-Al alloys by a two-parameter fit; thus a single power-law extrapolation for the reflectance was used.

The spectral dependence of n and k for pure gold is shown in Figs. 3 and 4, as well as values of n and k reported by other investigators.[10–13] In each case, the sample was an evaporated film measured at room temperature. The present studies differ in that all our films were annealed. Other differences are the experimental method used and the sample environment. Optical constants shown in Figs. 3 and 4 and reported by other investigators were determined by ellipsometry or multiple-angle reflectances, but not by use of the Kramers–Kronig equations and normal-incidence reflectance. Also, their samples were exposed to pressures of 10^{-6} Torr or higher. In view of these differences, agreement between their values and ours is good.

A number of optical functions of more direct

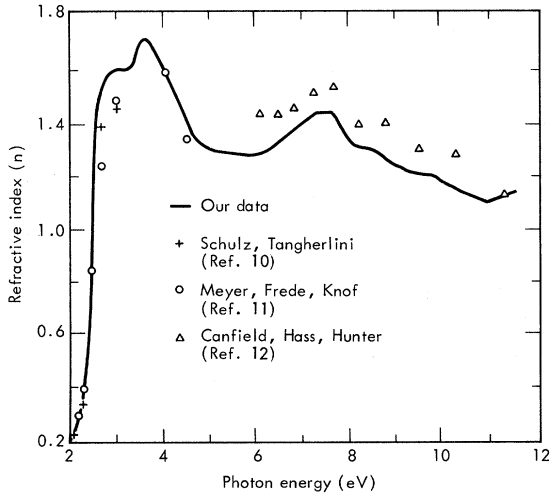

FIG. 3. Refractive index vs photon energy for gold.

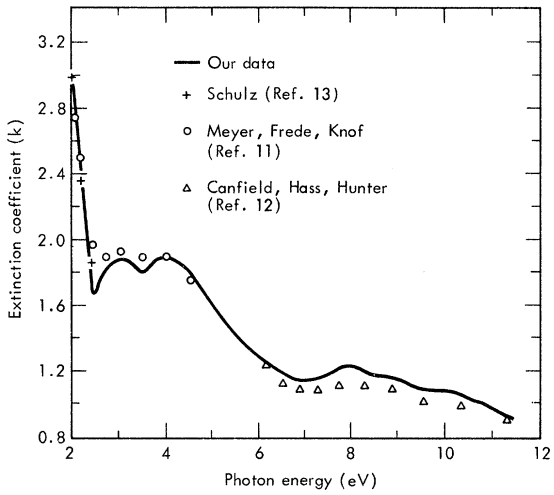

FIG. 4. Extinction coefficient vs photon energy for gold.

physical interest were calculated using the n and k values obtained from an analysis of reflectance data. These are shown graphically in Figs. 5–10.

IV. DISCUSSION

Structure in the dielectric function can best be discussed with the help of Fig. 11, which identifies the symmetry points in the fcc Brillouin zone, and the nonrelativistic band structure of gold shown in Fig. 12. The peak in ϵ_2 at 3.09 eV for pure gold is associated with the transition $L_3 \rightarrow L_2$, from the d band to the Fermi level near L.[7] Pells and

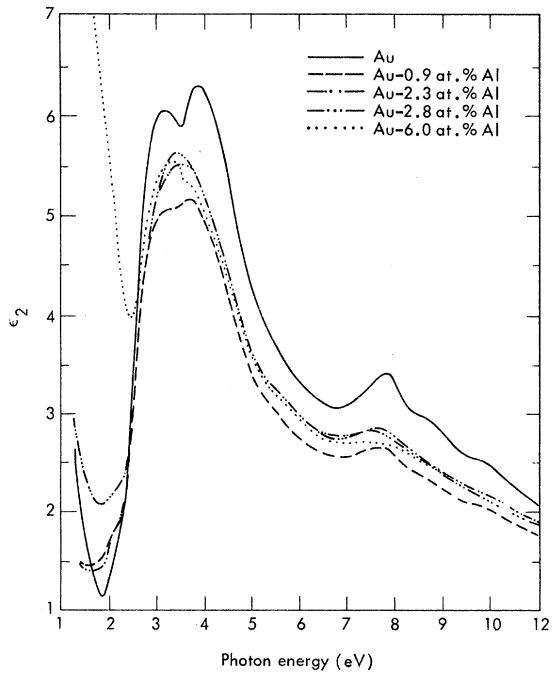

FIG. 6. ϵ_2 vs photon energy for gold and gold-aluminum at 300 °K.

Shiga[14] associate the 3.77-eV peak with $L_{2'} \rightarrow L_1^u$, and the 4.57-eV shoulder tentatively with $X_5 \rightarrow X_{4'}$. Erlbach and Beaglehole[15] associate the strong peak at 7.87 eV with $X_1 \rightarrow X_{4'}$. The two weaker peaks at 8.67 and 9.70 eV have apparently not been previously discussed. However, Fong[16] has informed

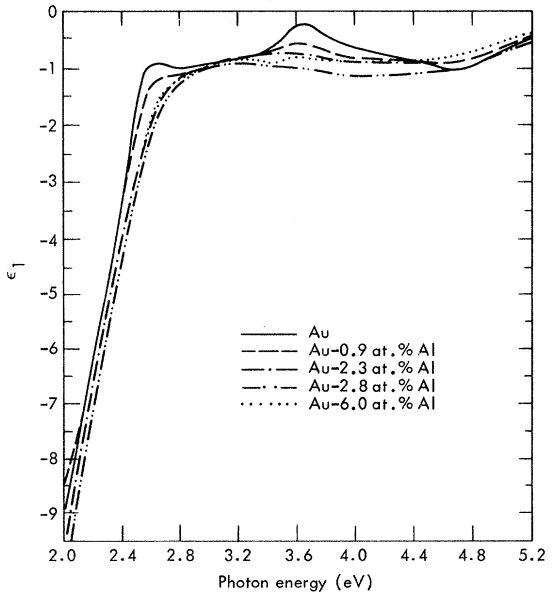

FIG. 5. ϵ_1 vs photon energy for gold and gold-aluminum at 100 °K.

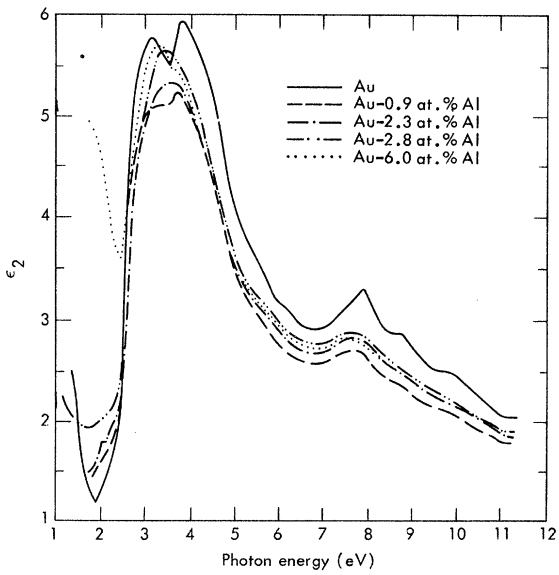

FIG. 7. ϵ_2 vs photon energy for gold and gold-aluminum at 100 °K.

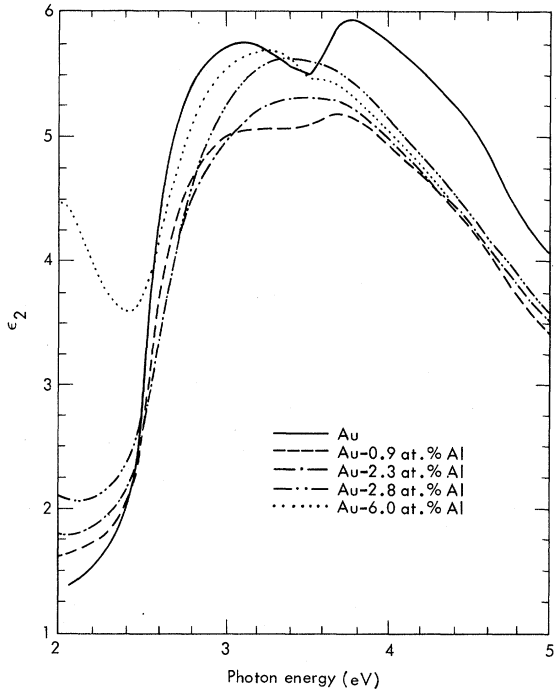

FIG. 8. Low-energy structures in ϵ_2 for gold and gold-aluminum at 100 °K.

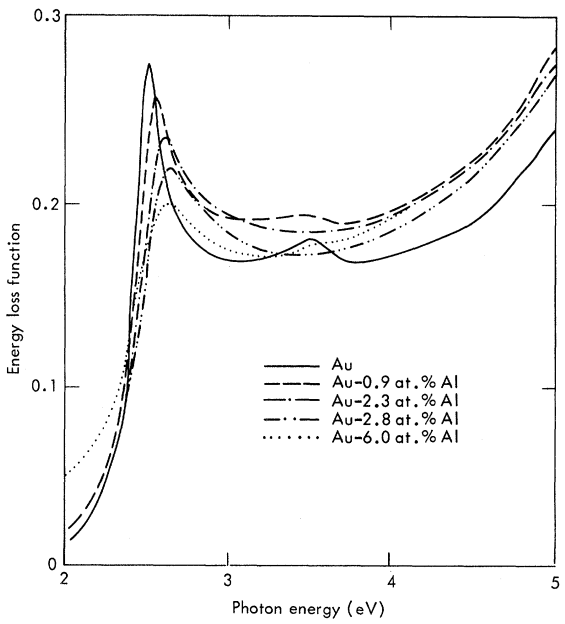

FIG. 10. Energy-loss function vs photon energy for gold and gold-aluminum at 100 °K.

us that calculations using the empirical pseudopotential method show that the structure at 8.67 eV arises mainly from interband transitions 1→6 and 2→6 and the structure at 9.7 eV arises from interband transitions 1→6, 2→6, and 3→7. These transitions occur over large regions of the Brillouin zone, not at the Fermi surface where the sixth band cuts the Fermi surface. These assignments agree with the conclusions of Christensen and Seraphin[17] that structure in the static reflection curves for pure gold is not related to critical points in the band structure.

How consistent are these assignments with the data on Au-Al alloys? It is somewhat difficult to follow all the shifts in peaks upon alloying; some are damped and broadened. Nonetheless, a care-

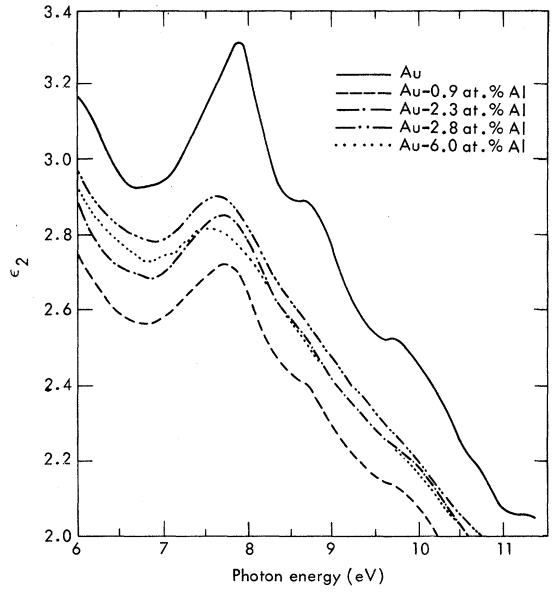

FIG. 9. High-energy structures in ϵ_2 for gold and gold-aluminum at 100 °K.

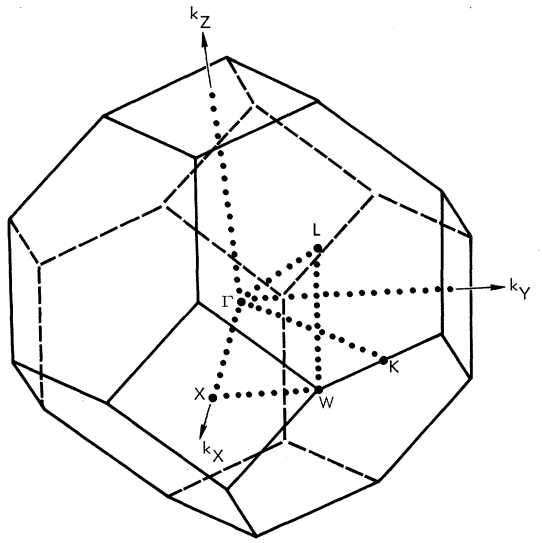

FIG. 11. Symmetry points in the fcc Brillouin zone.

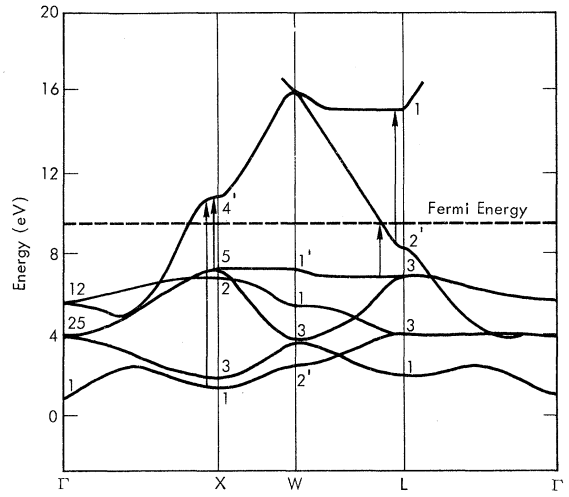

FIG. 12. Nonrelativistic band structure of gold with important transitions indicated. (Based on Christensen and Seraphin, Ref. 16.)

ful study of the data indicates that the $L_3 \rightarrow L_{2'}$ peak moves to higher energies, whereas the $X_5 \rightarrow X_{4'}$, $L_{2'} \rightarrow L_1^u$, and $X_1 \rightarrow X_{4'}$ structures move to lower energies with increasing aluminum concentration. The peaks at 8.67 and 9.70 eV are unchanged. Because addition of aluminum increases the electron concentration, the Fermi level might be raised by alloying. Then one would expect to see the observed shifts in $L_3 \rightarrow L_{2'}$ and $L_{2'} \rightarrow L_1^u$. However, $X_5 \rightarrow X_{4'}$ and $X_1 \rightarrow X_{4'}$ are from well below to well above the Fermi level and should remain unchanged unless there is some shift of the conduction bands with respect to the d bands. Inasmuch as the 8.67- and 9.70-eV peaks are unchanged, and they must certainly be from below the Fermi level to above it, any change in the conduction bands with respect to the d bands must be selective. In particular, it seems that there must be a downward shift of $X_{4'}$ with respect to the d bands. The shift is, in fact, quite large; it is about 0.15 eV/at.% aluminum.

Clearly, the rigid-band model is inadequate to describe an alloy in which there are selective shifts in the conduction band with respect to the d bands. It is more difficult to draw conclusions concerning the applicability of the rigid-band model for states near the Fermi energy. Except for pure gold and the alloy containing 6 at.% aluminum, the peak corresponding to the $L_3 \rightarrow L_{2'}$ transition is not well defined. However, assuming that the $L_3 \rightarrow L_{2'}$ peak for the 6 at.% aluminum alloy provides a fair description of what happens for this alloy system, we can make some estimates concerning the validity of the rigid-band model. The shift in energy expected on the basis of the rigid-band model is given by

$$\Delta E = (Z-1) n_a \, C/\rho(E_F) \,, \tag{3}$$

where Z is the valence of the solute (3 for aluminum), n_a is the number density of atoms, C is the solute (aluminum) concentration, and $\rho(E_F)$ is the electronic density of states at the Fermi energy. For the gold alloy containing 6 at.% aluminum, using $\rho(E_F)$ as obtained from heat-capacity measurements,[18] the calculated shift is 0.36 eV. Since band calculations show the d band to be rather insensitive to the small changes in lattice potential expected in dilute alloys, the experimental shift of 0.18 eV suggests that one of the two extra valence electrons introduced by substituting aluminum for gold remains fairly localized at the solute site. Thus, just as was found for Ag-Al alloys, it appears that neither the rigid-band model, which predicts a change in Fermi level corresponding to just filling up empty states in a fixed band structure, nor the Friedel model of localized states, which predicts no change in Fermi level, agrees with experimental results. However, just as for the Ag-Al alloys, it is possible that part or all of the shift in the $L_3 \rightarrow L_{2'}$ peak arises from smearing of the d-band edge by increased lifetime broadening. Then the d bands could be stationary, in agreement with Friedel's theory. Also, since heat-capacity measurements overestimate $\rho(E_F)$, the shift in energy calculated from Eq. (3) should perhaps be larger. This would further increase the discrepancy with the rigid-band model.

It appears, then, that the rigid-band model provides an unsatisfactory description of α-phase Au-Al alloys. They might be described reasonably well by the Friedel model. However, the best description appears to be that of Stern,[4,5] who shows that alloys of noble metals have unique electronic properties because of the large separation between the highest filled bands and the higher unoccupied bands. In particular, for polyvalent impurities such as aluminum, the shielding charge is necessarily spread farther than calculated on the basis of free-electron shielding in the Thomas-Fermi model. As Stern shows, this follows from the theorem that in a completely filled band there are exactly two electrons around every atom, whether it is the impurity atom or the host atom. It is consistent with the present studies, which suggest that each aluminum atom has one of the two extra valence electrons highly localized, whereas the other electron is nonlocalized and contributes to a shift in Fermi level just half that to be expected for the simple rigid-band model.

ACKNOWLEDGMENT

We wish to thank C. Y. Fong for his helpful comments.

*Work performed under the auspices of the U. S. Atomic Energy Commission.

†Fannie and John Hertz Foundation Fellow. Present address: Johns Hopkins Applied Physics Laboratory, Silver Spring, Md. 20190.

[1]G. B. Irani, T. Huen, and F. Wooten, Phys. Rev. B 3, 2385 (1971).

[2]N. F. Mott and H. Jones, *The Theory of the Properties of Metals and Alloys* (Dover, New York, 1958), pp. 170–174.

[3]J. Friedel, Advan. Phys. 3, 446 (1954).

[4]E. A. Stern, Phys. Rev. 157, 544 (1967).

[5]E. A. Stern, Phys. Rev. 188, 1163 (1969).

[6]T. Huen, G. B. Irani, and F. Wooten, Appl. Opt. 10, 552 (1971).

[7]B. Cooper, H. Ehrenreich, and H. R. Philipp, Phys. Rev. 138, A494 (1965).

[8]H. Ehrenreich and H. R. Philipp, Phys. Rev. 128, 1622 (1961).

[9]R. Haensel, C. Kunz, T. Sasaki, and B. Sonntag, Appl. Opt. 7, 301 (1968).

[10]L. Schulz and F. Tangherlini, J. Opt. Soc. Am. 44, 362 (1954).

[11]E. Meyer, H. Frede, and H. Knof, J. Appl. Phys. 38, 3682 (1967).

[12]L. R. Canfield, G. Hass, and W. R. Hunter, J. Phys. (Paris) 25, 124 (1964).

[13]L. Schulz, J. Opt. Soc. Am. 44, 357 (1954).

[14]G. P. Pells and M. Shiga, J. Phys. C 2, 1835 (1969).

[15]E. Erlbach and D. Beaglehole, in *Third Materials Research Symposium, Electronic Density of States*, Natl. Bur. Std. Misc. Publ. (U. S. GPO, Washington, D. C., 1971), pp. 545–555.

[16]C. Y. Fong (private communication).

[17]N. E. Christensen and B. O. Seraphin, Phys. Rev. B 4, 3321 (1971). The structures indentified by Pells and Shiga (Ref. 14) as $L_{2'} \rightarrow L_1^u$ and $X_5 \rightarrow X_{4'}$ are labeled $L_4^- \rightarrow L_4^+$ and $X_7^{+2} \rightarrow X_6^-$ in the relativistic calculations of Christensen and Seraphin (CS). Strictly speaking, the Pells – Shiga results for $X_5 \rightarrow X_4'$ correspond to $X_2 \rightarrow X_4'$ in CS. In the nonrelativistic case X_5 has higher energy than X_2. X_7^{+2} is derived from X_2. The onset of the peak in ϵ_2 at 3.09 eV is identified by CS as interband transition $5 \rightarrow 6$ at the Fermi surface.

[18]L. L. Issacs, J. Chem. Phys. 43, 307 (1965).

PHYSICAL REVIEW B VOLUME 6, NUMBER 8 15 OCTOBER 1972

Perturbed-Angular-Correlation Studies of the Quadrupole Interactions of ^{111}Cd in Different Metallic Environments and the Electric Quadrupole Moment of the 247-keV State

E. Bodenstedt,* U. Ortabasi,† and W. H. Ellis
Department of Nuclear Engineering Sciences, University of Florida, Gainesville, Florida 32601

(Received 28 December 1971)

The quadrupole interactions of the 247-keV state of ^{111}Cd populated in the decay of ^{111}In have been studied by time-dependent perturbed-angular-correlation measurements in environments of metallic indium and indium-cadmium alloys. Periodic undamped-spin-rotation curves were observed which prove that in both cases the axial-asymmetry parameter of the electric field gradient is close to zero and the spread of the interaction frequencies is negligibly small. The temperature dependence of the interaction frequencies in metallic indium is quite strong but deviates only slightly from that observed by Hewitt and Taylor for the stable indium isotopes in the same environment using the nuclear-quadrupole-resonance (NQR) technique. We draw the conclusion that the localized-moment contribution of the conduction electrons to the electric field gradient must be small in this case, and by using the results of Hewitt and Taylor for a calibration of the effective electric field gradient, we derived for the electric quadrupole moment of the 247-keV state of ^{111}Cd $Q_{5/2} = +0.44 \pm 0.07 \times 10^{-24}$ cm^2. The quadrupole interactions in the indium-cadmium alloy (0.94 at.% indium) were found to be an order of magnitude larger than in indium. This was expected because of the anomalously large c/a crystal-axes ratio of the hexagonal-close-packed (hcp) lattice of cadmium. The observed temperature dependence gives interesting information about the role of the conduction electrons as well as about the phase diagram of the cadmium-indium system.

I. INTRODUCTION

Electric quadrupole interactions of nuclei in metals can be studied by different techniques. The nuclear quadrupole resonance (NQR) measures the quadrupole splitting of nuclear ground states. Mössbauer spectroscopy observes the quadrupole splitting of the excited state and the ground state of the investigated γ transition, and finally, time-dependent perturbed-angular-correlation (TDPAC) measurements determine the quadrupole interaction in an excited nuclear state, the intermediate state of the γ-γ cascade.

The results of NQR experiments are usually used to study solid-state effects, e.g., the structure of metals and metal alloys, and the contribution of the conduction band to the effective electric field gradient.